ON THE STRUCTURE OF BOAT-SHAPED HEXALEAD(II) CATIONS WITH OH BRIDGES

Martin BREZA[1,*] and Stanislav BISKUPIČ[2]

Department of Physical Chemistry, Slovak Technical University, SK-812 37 Bratislava, Slovak Republic; e-mail: [1] breza@cvt.stuba.sk, [2] biskupic@cvt.stuba.sk

Received May 28, 2004
Accepted October 11, 2004

In the memory of Professor Ladislav Turi-Nagy (1948–2003).

Using Hartree–Fock, B3LYP, and MP2 treatments, the optimal boat-shaped geometries and corresponding electronic structures of $[Pb_6O_m(\mu_3\text{-}OH)_n]^q$ complex cations with total charges $q = 12 - 2m - n$, $m = 0$ or 1, $n = 6$ or 8, are investigated. Whereas the $[Pb_6(\mu_3\text{-}OH)_6]^{6+}$ cation is unstable, the remaining structures preserve C_{2v} symmetry. Direct Pb–Pb interactions are weakly antibonding in all the systems under study. The clusters are held together exclusively by relatively weak Pb–O bonds. The effects of central O and two additional μ_3-OH bridges in $[Pb_6O(\mu_3\text{-}OH)_8]^{2+}$ are not fully cooperative. $[Pb_6O(\mu_3\text{-}OH)_6]^{4+}$ and $[Pb_6(\mu_3\text{-}OH)_8]^{4+}$ may coexist in water solutions in comparable concentrations.

Keywords: Lead(II) clusters; Hydroxo complexes; Molecular structure; Geometry optimizations; Ab initio calculations.

The water pollution by lead(II) compounds is of great importance due to their toxicity, but only few studies focussed on the structure of products of their hydrolysis. The formation and precipitation of $[Pb(II)_x(O,OH)_y]^{n+}$ species in aqueous systems has many important implications. Structural characterization of these compounds in solutions is important for understanding the mechanism of lead transport in natural systems.

According to precise potentiometric titration data[1], $[Pb_6(OH)_8]^{4+}$ complex cations are the largest ones formed in hydrolysis of lead(II) in perchlorate and nitrate solutions over a broad concentration and pH range. X-ray diffraction studies[2] of concentrated alkaline solutions of lead(II) perchlorate with the molar ratio OH/Pb 4:3 indicate that each lead atom in this species is surrounded by four other Pb atoms on average, at a distance of about 3.85×10^{-10} m. Two more distances of lower frequencies occur at 6.37×10^{-10} and 7.1×10^{-10} m. No attempt has been made to locate the oxygen atoms, although the shortest Pb–O distances between 2×10^{-10} and

doi:10.1135/cccc20042055

3×10^{-10} m are clearly indicated in the radial distribution curves. Unfortunately, the solution X-ray data cannot be used for more definite conclusions about the oxygen positions.

Additional information may be deduced from the analogy with known crystal structures. Clusters with composition $[Pb_6O(OH)_6]$ were found in both polymorphs[3,4] of $[Pb_6O(OH)_6](ClO_4)_4 \cdot H_2O$ and in $[Pb_6O(OH)_6](ReO_4)_4 \cdot H_2O$ (lit.[5]). The six Pb atoms in $[Pb_6O(OH)_6]^{4+}$ occupy the vertices of three distorted Pb_4 tetrahedra connected by common faces (Fig. 1). On the other hand, in $Pb_3O_2(OH)_2$, a topologically different and electrostatically neutral cluster, $[Pb_6O_4(OH)_4]$, has been found[6]; it can be described as an almost regular Pb_6 octahedron whose eight triangular faces are "topped" by O atoms or OH groups. Isolated $[Pb_6O_2]$ clusters (two OPb_4 tetrahedra sharing an edge) occur in Pb_3UO_6 (lit.[7]).

Since the potentiometric measurements cannot differentiate between one O^{2-} and two OH^- groups, the presence of $[Pb_6(OH)_8]^{4+}$ as well as $[Pb_6O(OH)_6]^{4+}$ clusters in perchlorate solutions is possible[2]. Due to the width of the peaks in the radial distribution function at large interatomic distances, the X-ray measurements cannot be used to decide which of the above two clusters is most related to the species occurring in solution. In analogy with the crystal structures of $[Pb_6O(\mu_3\text{-}OH)_6](XO_4)_4 \cdot H_2O$, (X = Cl or Re)[3–5], Johansson and Olin[2] have assumed a boat-shaped arrangement of six lead atoms which can be considered as three face-sharing Pb_4 tetrahedra with central oxide ion inside the central Pb_4 tetrahedron and six μ_3-OH bridges over external faces of the remaining ones (Fig. 2).

Isolated $[Pb_4(\mu_3\text{-}OH)_4]^{4+}$ complex cations (without central oxide atom) are present in solution[2,8] as well as in the solid $[Pb_4(\mu_3\text{-}OH)_4]_3(CO_3)(ClO_4)_{10} \cdot 6H_2O$ (lit.[9]) and $[Pb_4(\mu_3\text{-}OH)_4](ClO_4)_4 \cdot 2H_2O$ (lit.[10]) structures. The same cluster

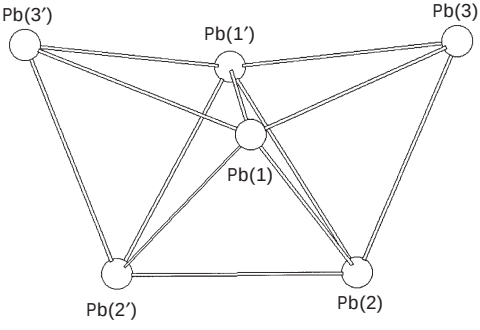

FIG. 1
Arrangement and notation of Pb atoms in boat-shaped hexalead(II) complexes

occupies the sodalite cage[11] in zeolite X and is present in maricopaite[12], $Pb_7Ca_2[Al_{12}Si_{36}(O,OH)_{100}]\cdot n(H_2O,OH)$, $n \approx 32$ and in $[Pb_4(OH)_4](NO_3)_4$ (lit.[8]).

Hexalead(II) solid structures of α- and β-forms[3,4] of $[Pb_6O(\mu_3\text{-}OH)_6](ClO_4)_4\cdot H_2O$ as well as $[Pb_6O(\mu_3\text{-}OH)_6](ReO_4)_4\cdot H_2O$ (lit.[5]) contain central oxo-centered OPb_4 as well as lateral empty Pb_4 tetrahedra. On the other hand, some solid crystals obtained from alkaline lead(II) solutions contain infinite $[O_2Pb_3]$ double chains of exclusively oxo-centered OPb_4 tetrahedra[13] (each tetrahedron has two topologically distinct Pb vertices: two "outer" Pb atoms are shared by two OPb_4 tetrahedra, whereas the other two "inner" Pb ones are shared by four OPb_4 tetrahedra). This implies that the Pb_4 tetrahedra sharing two and more faces are not stabilized by "outside" μ_3-OH bridges and one of these bridges is converted to "inner" oxide anion. The resulting OPb_4 tetrahedra cannot contain any additional μ_3-OH bridges.

Based on very simple quantum-chemical models, Bengtsson and Hoffman[14] concluded that dilead structure units are stabilized by partial Pb–Pb bonding induced by bridging hydroxide ions. The strongest Pb–Pb bonds were deduced in complexes with predominantly ionic lead–anion interactions. They concluded that larger hydroxo/oxo clusters in aqueous solutions also seem to be stabilized by partial Pb–Pb bonding whereas in the solid structures of isolated hydroxo/oxo clusters Pb–O bonding predominates (only long Pb–Pb contacts have been found). The concept of direct Pb–Pb bonding is used also in chemistry textbooks[15].

On the other hand, semiempirical quantum-chemical studies[16] indicate that the individual Pb atoms are bonded only via OH bridges due to vanishing Pb–Pb bonds. The stability of individual isomers increases with the

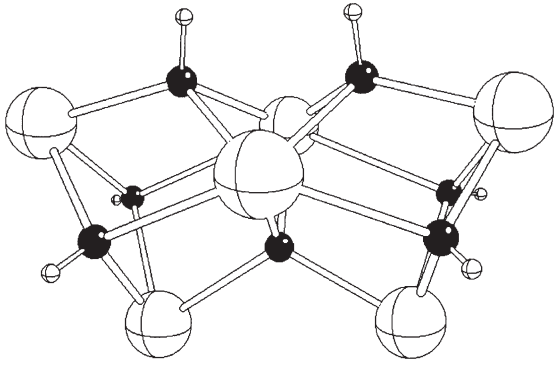

FIG. 2
Geometry of $[Pb_6O(\mu_3\text{-}OH)_6]^{4+}$ cluster

number of OH bridges. Moreover, an ab initio MP2 study on dilead hydroxo complexes[17] indicates a weakly repulsive character of mutual Pb(II)–Pb(II) interactions. Other MP2 studies are restricted to the structure and vibrational spectra of $[Pb_4(OH)_4]^{4+}$ (lit.[18]) and $[Pb_6O(OH)_6]^{4+}$ (lit.[19]) clusters.

The aim of this study is ab initio investigation of stable geometries and corresponding electronic structure of boat-shaped hexalead(II) clusters with various numbers of hydroxide bridges and the role of the central oxygen atom in these complexes. This might be helpful for understanding the mechanisms of their formation in aqueous solutions and subsequent crystallization in real solid systems.

CALCULATIONS

Using Gaussian 94 program package[20], the optimal geometries of tetrahedral $[Pb_6(\mu_3\text{-}OH)_n]^q$ and $[Pb_6O(\mu_3\text{-}OH)_n]^{q-2}$ complex cations with total charges $q = 12 - n$, $n = 6$ or 8, are investigated within standard restricted Hartree–Fock (HF), B3LYP and MP2 treatments[21,22] using standard accuracy parameters. Dunning–Huzinaga full double zeta basis sets with polarization functions have been used for O and H atoms[23] whereas the LANL2DZ effective core potential and (3s,4p,1d)/[2s,3p,1d] basis set[24,25] with diffuse and polarization functions[25,26] have been used for Pb atoms. Electron structure parameters have been evaluated in terms of Mulliken population analysis (gross atomic charges, overlap populations).

RESULTS AND DISCUSSION

Lead atoms numbering of the hexalead boat-shaped complex cations under study is given in Fig. 1. The oxygen atom located in the center of Pb(1)Pb(1′)Pb(2)Pb(2′) tetrahedron is denoted as O(central) (see, e.g., Fig. 2) whereas the remaining oxygen and hydrogen atoms of bridging OH are labeled according to the bonded lead atoms (e.g., O(11′3) atom is bonded to Pb(1), Pb(1′) and Pb(2) whereas H(11′3) is bonded to O(11′3)).

Our study began with geometry optimization of $[Pb_6O(\mu_3\text{-}OH)_6]^{4+}$ in experimental geometry (see Fig. 2). The starting geometry of the remaining complex cations was obtained by adding two μ_3-OH bridges ($[Pb_6O(\mu_3\text{-}OH)_8]^{2+}$) or removing O(central) atom ($[Pb_6(\mu_3\text{-}OH)_6]^{4+}$) or both ($[Pb_6(\mu_3\text{-}OH)_8]^{6+}$).

Our results indicate that the $[Pb_6(\mu_3\text{-}OH)_6]^{6+}$ system is unstable, i.e. splits into two parts, whereas the remaining structures preserve the C_{2v} symmetry (the only exception is the Hartree–Fock-optimized $[Pb_6(\mu_3\text{-}OH)_8]^{4+}$ system –

its instability illustrates the necessity of the correlation effects inclusion). This implies that primed atoms are symmetry related with the unprimed ones by mirror planes (Fig. 1). The geometry parameters of the stable systems (Figs 2–4) are described in Tables I–III and compared with experimental X-ray interatomic distances (the angles for solvent are unknown[2], the averaged angles for solids are not presented due to very large standard deviations[3–5]). Our structure data for $[Pb_6O(\mu_3\text{-}OH)_6]^{4+}$ agree with the results of Jensen's MP2 calculations using SDD basis sets (differences of interatomic distances below 0.05×10^{-10} m except O(113) atoms positions)[19] and are in reasonable agreement with corresponding solution[2] as well as averaged solid structure[3–5] data (MP2 interatomic distances are within standard deviations except Pb(1)–Pb(1′) and Pb(2)–Pb(2′), this affects also Pb(2)–Pb(3′) and Pb(3)–Pb(3′) distances).

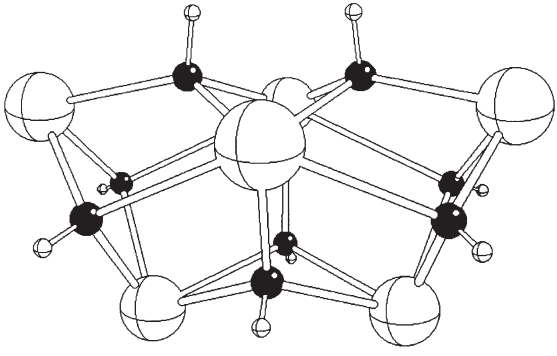

FIG. 3
Geometry of $[Pb_6(\mu_3\text{-}OH)_8]^{4+}$ cluster

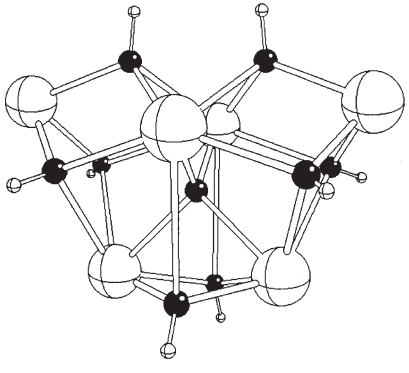

FIG. 4
Geometry of $[Pb_6O(\mu_3\text{-}OH)_8]^{2+}$ cluster

TABLE I
Selected structure data for $[Pb_6O(\mu_3\text{-}OH)_6]^{4+}$ complex cation (Fig. 2)

Interatomic distances 10^{-10} m	Calculated			X-ray experiment		Angles, °	Calculated		
	HF	B3LYP	MP2	solution[2]	solid[a]		HF	B3LYP	MP2
Pb1–O11′3	2.413	2.454	2.45	≈2.6	2.4(1)	Pb1–O11′3–Pb1′	87.0	87.2	87.9
Pb1–O123	2.941	2.894	2.824	≈2.6	2.7(1)	Pb1–O11′3–Pb3	116.5	115.7	115.8
Pb1–Ocentral	2.235	2.289	2.303	≈2.6	2.28(4)	Pb1–O123–Pb2	94.8	95.9	97.1
Pb2–O123	2.225	2.257	2.269	≈2.6	2.31(6)	Pb1–O123–Pb3	101.5	102.4	103.7
Pb2–Ocentral	2.404	2.378	2.357	≈2.6	2.31(5)	Pb1–Ocentral–Pb1′	97.0	95.4	95.5
Pb3–O11′3	2.356	2.351	2.331	≈2.6	2.30(3)	Pb1–Ocentral–Pb2	111.4	111.1	110.7
Pb3–O123	2.289	2.307	2.318	≈2.6	2.30(5)	Pb2–O123–Pb3	107.3	105.8	106.0
Pb1–Pb1′	3.347	3.387	3.409	≈3.85	3.44(2)	Pb2–Ocentral–Pb2′	113.2	115.5	116.5
Pb1–Pb2	3.833	3.848	3.835	≈3.85	3.79(7)	O11′3–Pb1–O11′3′	71.3	70.4	69.3
Pb1–Pb3	4.070	4.070	4.055	≈3.85	3.99(9)	O11′3–Pb1–O123	63.8	64.1	64.0
Pb2–Pb2′	4.013	4.020	4.007	≈3.85	3.82(7)	O11′3–Pb1–O12′3′	128.3	128.2	127.1
Pb2–Pb3	3.635	3.640	3.663	≈3.85	3.69(4)	O11′3–Pb1–Ocentral	76.7	77.5	77.4
Pb2–Pb3′	6.542	6.543	6.530	≈6.37	6.39(8)	O11′3–Pb3–O123	76.2	75.9	74.3
Pb3–Pb3′	7.372	7.352	7.295	≈7.14	7.13(2)	O123–Pb1–O12′3	131.7	132.2	133.1
O11′3–H11′3	0.954	0.977	0.981			O123–Pb1–Ocentral	69.6	69.7	69.8
O123–H123	0.955	0.976	0.980			O123–Pb2–O1′23	73.3	74.1	73.5
						O123–Pb2–Ocentral	81.1	80.7	77.5
						O123–Pb3–O1′23	70.9	72.3	71.8
						Pb1–O11′3–H11′3	113.2	113.2	112.6
						Pb1–O123–H123	112.7	115.0	114.7
						Pb2–O123–H123	119.2	117.9	116.9
						Pb3–O11′3–H11′3	109.3	110.1	110.6
						Pb3–O123–H123	117.8	116.9	116.0

[a] Averaged interatomic distances from $[Pb_6O(\mu_3\text{-}OH)_6](XO_4)_4 \cdot H_2O$ structure data, X = Cl [3,4], Re [5] (standard deviation in parentheses, its order corresponds to the order of the last valid digit).

TABLE II
Selected structure data for $[Pb_6(\mu_3\text{-}OH)_8]^{4+}$ complex cation (Fig. 3)

Distances 10^{-10} m	B3LYP	MP2	Angles, °	B3LYP	MP2
Pb1–O11′3	2.412	2.452	Pb1–O11′3–Pb1′	101.3	101.2
Pb1–O122′	2.241	2.293	Pb1–O11′3–Pb3	121.1	118.7
Pb1–O123	3.439	3.046	Pb1–O122′–Pb2	118.8	115.6
Pb2–O122′	2.624	2.512	Pb1–O123–Pb2	92.2	97.8
Pb2–O123	2.273	2.324	Pb1–O123–Pb3	98.9	103.4
Pb3–O11′3	2.593	2.410	Pb2–O122′–Pb2′	102.0	106.7
Pb3–O123	2.204	2.246	Pb2–O123–Pb3	107.5	106.9
Pb1–Pb1′	3.729	3.789	O11′3–Pb1–O11′3′	72.4	67.4
Pb1–Pb2	4.192	4.069	O11′3–Pb1–O123	57.8	59.3
Pb1–Pb3	4.362	4.183	O11′3–Pb1–O12′3′	120.0	119.0
Pb2–Pb2′	4.077	4.031	O11′3–Pb3–O123	75.9	72.9
Pb2–Pb3	3.612	3.671	O122′–Pb1–O11′3	92.3	95.3
Pb2–Pb3′	6.722	6.593	O122′–Pb1–O123	61.1	63.9
Pb3–Pb3′	7.878	7.440	O122′–Pb2–O123	77.3	73.5
O11′3–H11′3	0977	0.981	O122′–Pb2–O1′23	111.6	108.2
O122′–H122′	0978	0.982	O122′–Pb1–O12′3′	122.0	127.3
O123–H123	0975	0.980	O123–Pb2–O1′23	71.2	71.0
			O123–Pb3–O1′23	73.8	73.8
			Pb1–O11′3–H11′3	104.9	104.7
			Pb1–O122′–H122′	105.0	103.1
			Pb1–O123–H123	111.6	113.4
			Pb2–O122′–H122′	105.5	107.7
			Pb2–O123–H123	120.2	115.8
			Pb3–O11′3–H11′3	101.5	107.4
			Pb3–O123–H123	120.6	117.3

TABLE III
Selected structure data for $[Pb_6O(\mu_3\text{-}OH)_8]^{2+}$ complex cation (Fig. 4)

Distances 10^{-10} m	HF	B3LYP	MP2	Angles, °	HF	B3LYP	MP2
Pb1–O11′3	2.549	2.553	2.548	Pb1–O11′3–Pb1′	84.0	84.8	85.7
Pb1–O122′	3.343	3.359	3.254	Pb1–O11′3–Pb3	108.9	108.5	108.9
Pb1–O123	2.597	2.594	2.575	Pb1–O122′–Pb2	81.8	81.9	83.4
Pb1–Ocentral	2.101	2.135	2.135	Pb1–O123–Pb2	91.2	92.0	92.9
Pb2–O122′	2.255	2.277	2.292	Pb1–O123–Pb3	108.0	107.8	103.8
Pb2–O123	2.660	2.594	2.611	Pb1–Ocentral–Pb1′	108.5	107.4	108.5
Pb2–Ocentral	2.365	2.357	2.344	Pb1–Ocentral–Pb2	114.3	114.6	114.0
Pb3–O11′3	2.191	2.216	2.213	Pb2–O123–Pb3	104.2	103.4	103.8
Pb3–O123	2.169	2.191	2.201	Pb2–O122′–Pb2′	96.0	94.8	94.5
Pb1–Pb1′	3.410	3.441	3.466	Pb2–Ocentral–Pb2′	90.2	90.7	91.8
Pb1–Pb2	3.756	3.782	3.758	O11′3–Pb1–O11′3′	65.9	65.5	64.9
Pb1–Pb3	3.863	3.874	3.879	O11′3–Pb1–O122′	116.9	117.0	116.9
Pb2–Pb2′	3.351	3.353	3.367	O11′3–Pb1–O123	64.7	65.4	65.2
Pb2–Pb3	3.823	3.819	3.795	O11′3–Pb1–O12′3′	127.0	127.0	126.0
Pb2–Pb3′	6.132	6.136	6.126	O11′3–Pb1–	75.7	75.8	74.9
Pb3–Pb3′	6.860	6.880	6.871	O11′3–Pb3–O123	78.3	78.2	77.4
O11′3–H11′3	0.948	0.971	0.973	O122′–Pb1–O123	71.7	71.0	70.8
O122′–H122′	0.949	0.971	0.974	O122′–Pb1–	49.8	49.6	50.3
O123–H123	0.949	0.971	0.974	O122′–Pb2–O123	91.4	90.3	88.2
				O122′–Pb2–O1′23	135.8	135.8	134.2
				O122′–Pb2–	67.1	67.0	65.4
				O123–Pb1–O1′23	142.1	140.8	140.0
				O123–Pb1–Ocentral	74.7	74.3	73.7
				O123–Pb2–O1′23	65.4	66.4	67.0
				O123–Pb2–Ocentral	69.6	69.7	69.9
				O123–Pb3–O1′23	83.1	83.5	81.8
				Pb1–O11′3–H11′3	116.7	117.2	116.9
				Pb1–O122′–H122′	135.0	139.8	139.4
				Pb1–O123–H123	117.8	118.5	118.2
				Pb2–O122′–H122′	124.3	122.3	121.5
				Pb2–O123–H123	114.3	114.9	114.2
				Pb3–O11′3–H11′3	117.0	116.3	115.7
				Pb3–O123–H123	117.6	116.6	116.2

Very low Pb–O–Pb angles (Tables I–III) are associated with longer Pb–O distances which indicate weaker Pb–O bonds. Shorter Pb(1)–Pb(1′), Pb(1)–Pb(2), Pb(1)–Pb(3) and Pb(3)–O(11′3) interatomic distances (and lower corresponding Pb–O–Pb angles) may be observed in the systems with O(central) atom. The presence of two additional μ_3-O(122′)H(122′) bridges is associated with shorter Pb(1)–O(123), Pb(1)–O(central) and Pb(3)–O(123) interatomic distances whereas the Pb(1)–Pb(1′) and Pb(2)–O(123) ones are longer. The presence of both O(central) and two μ_3-O(122′)H(122′) bridges in $[Pb_6O(\mu_3\text{-}OH)_8]^{2+}$ causes enormous elongation of Pb(1)–O(122′) bonds.

Despite being a rough approximation, the comparison of the energy data of the systems under study (Table IV) indicates that the reaction equilibria

$$[Pb_6O(\mu_3\text{-}OH)_8]^{2+} \rightarrow [Pb_6O(\mu_3\text{-}OH)_6]^{4+} + 2\ OH^- \qquad (1)$$

$$[Pb_6(\mu_3\text{-}OH)_8]^{4+} + 2\ OH^- \rightarrow [Pb_6O(\mu_3\text{-}OH)_8]^{2+} + H_2O \qquad (2)$$

should be shifted to the $[Pb_6O(\mu_3\text{-}OH)_8]^{2+}$ formation whereas the equilibrium

$$[Pb_6(\mu_3\text{-}OH)_8]^{4+} \rightarrow [Pb_6O(\mu_3\text{-}OH)_6]^{4+} + H_2O \qquad (3)$$

indicates comparable concentrations of both hexalead complex cations under normal conditions. These conclusions are valid for the total energies independent on the zero-point-energy (ZPE) corrections. Unfortunately, ZPE

TABLE IV
Energy characteristics of the systems under study (with and without ZPE correction)

Energy, a.u.	HF no	B3LYP no	MP2 no	HF yes	B3LYP yes
Total energy					
OH^-	–76.37245	–75.77055	–75.56978	–75.36342	–75.76225
H_2O	–76.04695	–76.44505	–76.24288	–76.02370	–76.42359
$[Pb_6O(\mu_3\text{-}OH)_6]^{4+}$	–546.04695	–550.16142	–548.51117	–546.72790	–550.07292
$[Pb_6(\mu_3\text{-}OH)_8]^{4+}$	–	–626.62532	–624.76300	–	–626.51308
$[Pb_6O(\mu_3\text{-}OH)_8]^{2+}$	–698.742615	–702.91119	–700.85513	–698.61991	–702.79746
Reaction energy					
Reaction (*1*)	1.17462	1.20868	1.20441	1.16517	1.20005
Reaction (*2*)	–	–1.18984	–1.19549	–	–1.18348
Reaction (*3*)	–	0.01884	0.00894	–	0.01657

corrections to MP2 energy data cannot be evaluated due to technical problems (very large complex cations with more than 220 orbitals).

The charge distribution (Tables V–VII) over Pb, O and H atoms depends on the total cluster charge but the highest negative charge is located at O(central) whereas the O(122′) charge is the least negative. O(central) causes higher polarity of Pb–O bonds. As in our previous studies[16,17], all Pb–Pb interactions are weakly antibonding and the clusters are held together exclusively by relatively weak Pb–O bonds (overlap populations below one third of those of O–H). O(central) is bonded to Pb stronger than OH bridges (compare overlap populations). The advantage of O(central) over two μ_3-O(122′)H(122′) bridges lies in stronger Pb(1)–O(123), Pb(2)–O(123) and Pb(3)–O(11′3) bonds (higher overlap populations). The effects of O(central) and two μ_3-O(122′)H(122′) bridges in $[Pb_6O(\mu_3\text{-}OH)_8]^{2+}$ are not fully cooperative (compare our previous conclusions[16] on contradicting bonding mechanisms of μ_3-OH and μ_2-OH bridges). Their absence is the reason for $[Pb_6O(\mu_3\text{-}OH)_6]^{6+}$ instability.

TABLE V
Electronic structure data for $[Pb_6O(\mu_3\text{-}OH)_6]^{4+}$ complex cation (Fig. 2)

Atomic charges	HF	B3LYP	MP2	Overlap populations	HF	B3LYP	MP2
Pb1	1.519	1.263	1.332	Pb1–O11′3	0.002	0.002	0.006
Pb2	1.525	1.279	1.337	Pb1–O123	0.029	0.067	0.043
Pb3	1.554	1.326	1.401	Pb1–Ocentral	0.036	0.069	0.065
O113	–1.063	–0.850	–0.923	Pb2–O123	0.005	0.023	0.057
O123	–1.068	–0.851	–0.922	Pb2–Ocentral	0.015	0.056	0.054
Ocentral	–1.340	–1.021	–1.066	Pb3–O11′3	0.008	0.043	0.034
H113	0.411	0.388	0.398	Pb3–O123	0.013	0.053	0.043
H123	0.427	0.404	0.416	Pb1–Pb1′	–0.051	–0.061	–0.046
				Pb1–Pb2	–0.024	–0.026	–0.022
				Pb1–Pb3	–0.032	–0.039	–0.012
				Pb2–Pb2′	–0.022	–0.023	–0.019
				Pb2–Pb3	–0.013	–0.015	–0.028
				O11′3–H11′3	0.325	0.308	0.295
				O123–H123	0.329	0.312	0.300

TABLE VI
Electronic structure data for $[Pb_6(\mu_3\text{-}OH)_8]^{4+}$ complex cation (Fig. 3)

Atomic charges	B3LYP	MP2	Overlap population	B3LYP	MP2
Pb1	1.232	1.333	Pb1–O11′3	0.050	0.034
Pb2	1.282	1.352	Pb1–O122′	0.074	0.050
Pb3	1.307	1.373	Pb1–O123	0.013	0.018
O11′3	–0.841	–0.911	Pb2–O122′	0.027	0.019
O122′	–0.835	–0.908	Pb2–O123	0.064	0.049
O123	–0.846	–0.918	Pb3–O11′3	0.029	0.025
H11′3	0.379	0.385	Pb3–O123	0.069	0.056
H122′	0.378	0.395	Pb1–Pb1′	–0.035	–0.025
H123	0.396	0.407	Pb1–Pb2	–0.013	–0.011
			Pb1–Pb3	–0.005	–0.007
			Pb2–Pb2′	–0.031	–0.021
			Pb2–Pb3	–0.047	–0.029
			O11′3–H11′3	0.302	0.290
			O122′–H122′	0.304	0.294
			O123–H123	0.315	0.301

TABLE VII
Electronic structure data for $[Pb_6O(\mu_3\text{-}OH)_8]^{2+}$ complex cation (Fig. 4)

Atomic charges	HF	B3LYP	MP2	Overlap population	HF	B3LYP	MP2
Pb1	1.489	1.179	1.265	Pb1–O11′3	0.007	0.033	0.023
Pb2	1.454	1.143	1.222	Pb1–O122′	0.009	0.016	0.016
Pb3	1.408	1.141	1.223	Pb1–O123	0.003	0.027	0.015
O11′3	–1.049	–0.836	–0.908	Pb1–Ocentral	0.033	0.077	0.072
O122′	–1.032	–0.826	–0.890	Pb2–O122′	0.023	0.066	0.055
O123	–1.045	–0.834	–0.906	Pb2–O123	–0.010	0.016	0.006
Ocentral	–1.383	–1.063	–1.118	Pb2–Ocentral	0.031	0.061	0.058
H11′3	0.375	0.347	0.361	Pb3–O11′3	0.037	0.075	0.068
H122′	0.375	0.375	0.375	Pb3–O123	0.053	0.092	0.081
H123	0.381	0.354	0.371	Pb1–Pb1′	–0.034	–0.047	–0.035
				Pb1–Pb2	–0.019	–0.023	–0.016
				Pb1–Pb3	–0.010	–0.015	–0.010
				Pb2–Pb2′	–0.037	–0.048	–0.037
				Pb2–Pb3	–0.016	–0.021	–0.016
				O11′3–H11′3	0.330	0.309	0.296
				O122′–H122′	0.337	0.312	0.300
				O123–H123	0.330	0.309	0.297

The various levels of calculations used in our study exhibit many similar trends mentioned above but many differences may be observed as well. The Hartree–Fock treatment gives higher atomic charges and weaker Pb–O bonds whereas O–H bonds are stronger than indicated by MP2 data. B3LYP data exhibit the same for O–H bonds whereas the reverse relations for atomic charges and Pb–O bonds may be observed. The existence of different trends at various levels of theory must be treated carefully (e.g. instability of $[Pb_6(\mu_3\text{-}OH)_8]^{4+}$ at Hartree–Fock level is an artifact).

CONCLUSIONS

It may be concluded that both $[Pb_6O(\mu_3\text{-}OH)_6]^{4+}$ (Fig. 2) and $[Pb_6(\mu_3\text{-}OH)_8]^{4+}$ (Fig. 3) as well as $[Pb_6O(\mu_3\text{-}OH)_8]^{2+}$ (Fig. 4) complex cations in boat-shaped geometries might be stable in real systems. The fact that $[Pb_6O(\mu_3\text{-}OH)_8]^{2+}$ has not been observed experimentally might be attributed to the environmental influence of water because polar solvents prefer the formation of cations with higher charges. This influence is of lower importance in the reaction (*3*) due to equal charges of both hexalead cations. Our results indicate that $[Pb_6O(\mu_3\text{-}OH)_6]^{4+}$ and $[Pb_6(\mu_3\text{-}OH)_8]^{4+}$ may coexist in water solutions in comparable concentrations. Solvent X-ray data[2] cannot reject any of these structures and the reliability of our MP2 results is confirmed by known solid X-ray structures[3–5]. In agreement with our previous studies[16,17], the crucial role of weak Pb–O bonds for the stability of the whole complex cation has been confirmed. Their absence causes instability of the structure due to mutual repulsion of lead atoms. Nevertheless, further theoretical studies on Pb–O bonding as well as on solvent effects are desirable for better understanding the problem as a whole.

The work reported in this paper has been funded by the Slovak Grant Agency (project No. 1/0052/03). We thank IBM Slovakia, Ltd. for computing facilities.

REFERENCES

1. a) Olin A.: *Acta Chem. Scand.* **1960**, *14*, 126; b) Olin A.: *Acta Chem. Scand.* **1960**, *14*, 814; c) Pajdowski L., Olin A.: *Acta Chem. Scand.* **1962**, *16*, 983; d) Hugel R.: *Bull. Soc. Chim. Fr.* **1964**, 1462; e) Hugel R.: *Bull. Soc. Chim. Fr.* **1965**, 968; f) Gyunner E. A., Tsareva A. I., Bakina N. B., Velmozhnyi I. S.: *Ukr. Khim. Zh.* **1978**, *44*, 348; g) Sylva R. N., Brown P. L.: *J. Chem. Soc., Dalton Trans.* **1980**, 1577; h) Cruywagen J. J., van de Water R. F.: *Talanta* **1993**, *40*, 1091; i) Arbatskii A. P., Benson V. V., Bolshakova E. V.: *Russian J. Phys. Chem.* **1995**, *69*, 1730.
2. Johansson G., Olin A.: *Acta Chem. Scand.* **1968**, *22*, 3197.

3. Spiro T. G., Templeton D. H., Zalkin A.: *Inorg. Chem.* **1969**, *8*, 856.
4. Olin A., Söderquist R.: *Acta Chem. Scand.* **1972**, *26*, 3505.
5. Haag-Bruhl C., Fuess H., Lightfoot P., Cheetham A. K.: *Acta Crystallogr., Sect. C: Cryst. Struct. Commun.* **1988**, *44*, 8.
6. Hill R. J.: *Acta Crystallogr., Sect. C: Cryst. Struct. Commun.* **1985**, *41*, 998.
7. Sterns M., Parise J. B., Howard C. J.: *Acta Crystallogr., Sect. C: Cryst. Struct. Commun.* **1986**, *42*, 1275.
8. Grimes S. M., Johnston S. R., Abrahams I.: *J. Chem. Soc., Dalton Trans.* **1995**, 2081.
9. Hong S.-H., Olin A.: *Acta Chem. Scand.* **1973**, *27*, 2309.
10. Hong S.-H., Olin A.: *Acta Chem. Scand., Ser. A* **1974**, *28*, 233.
11. Nardin G., Randaccio L., Zangrando E.: *Zeolites* **1995**, *15*, 684.
12. Rouse R. C., Peacor D. R.: *Am. Mineral.* **1994**, *79*, 175.
13. Kolitsch U., Tillmanns E.: *Mineral. Mag.* **2003**, *67*, 79; and references therein.
14. Bengtsson L. A., Hoffmann R.: *J. Am. Chem. Soc.* **1993**, *15*, 2666.
15. a) Cotton F. A., Wilkinson G.: *Advanced Inorganic Chemistry*, 5th ed., p. 297. Wiley, New York 1998; b) Ondrejovič G., Boča R., Jóna E., Langfelderová H., Valigura D.: *Anorganická chémia*, p. 366. Alfa, Bratislava 1993.
16. a) Breza M., Manová A.: *Collect. Czech. Chem. Commun.* **1995**, *60*, 527; b) Breza M., Manová A.: *Polyhedron* **1999**, *18*, 2085; c) Breza M., Manová A.: *Collect. Czech. Chem. Commun.* **1999**, *64*, 1269; d) Breza M., Manová A.: *Collect. Czech. Chem. Commun.* **2002**, *67*, 219.
17. Breza M., Biskupič S.: *Collect. Czech. Chem. Commun.* **2003**, *68*, 2377.
18. Jensen J. O.: *J. Mol. Struct. (THEOCHEM)* **2002**, *587*, 111.
19. Jensen J. O.: *J. Mol. Struct. (THEOCHEM)* **2003**, *635*, 11.
20. Frisch M. J., Trucks G. W., Schlegel H. B., Gill P. M. W., Johnson B. G., Robb M. A., Cheeseman J. R., Keith T. A., Petersson G. A., Montgomery J. A., Raghavachari K., Al-Laham M. A., Zakrzewski V. G., Ortiz J. V., Foresman J. B., Cioslowski J., Stefanov B. B., Nanayakkara A., Challacombe M., Peng C. Y., Ayala P. Y., Chen W., Wong M. W., Andres J. L., Replogle E. S., Gomperts R., Martin R. L., Fox D. J., Binkley J. S., Defrees D. J., Baker J., Stewart J. P., Head-Gordon M., Gonzales C., Pople J. A.: *Gaussian 94*, Revision D.1. Gaussian Inc., Pittsburgh (PA) 1995.
21. Becke A. D.: *J. Chem. Phys.* **1993**, *98*, 5648.
22. Møller C., Plesset M. S.: *Phys. Rev.* **1934**, *46*, 618.
23. Dunning T. H., Jr., Hay P. J. in: *Modern Theoretical Chemistry* (H. F. Schaefer III, Ed.), p. 1. Plenum, New York 1976.
24. Hay P. J., Wadt W. R.: *J. Chem. Phys.* **1985**, *82*, 299.
25. Basis sets were obtained from the Extensible Computational Chemistry Environment Basis Set Database, Version 2/12/03, as developed and distributed by the Molecular Science Computing Facility, Environmental and Molecular Sciences Laboratory which is part of the Pacific NorthWest Laboratory, P.O. Box 999, Richland, Washington 99352, USA, and funded by the U.S. Department of Energy. The Pacific NorthWest Laboratory is a multi-program laboratory operated by Battelle Memorial Institute for the U.S. Department of Energy under contract DE-AC06-76RLO 1830; http://www.emsl.pnl.gov/forms/basisform.html.
26. Check C. E., Faust T. O., Bailey J. M., Wright B. J., Gilbert T. M., Sunderlin L. S.: *J. Phys. Chem. A* **2001**, *105*, 8111.